fishes

MDPI

Article

Modeling the Ecological Consequences of an Open-Sea Nuclear Release on Resident and Migratory Marine Fish in the North Atlantic

Carmen Cortés [1,*] and Raúl Periáñez [2]

[1] Department Matemática Aplicada I, ETSIA, Universidad de Sevilla, Ctra Utrera Km 1, 41013 Sevilla, Spain
[2] Department Física Aplicada I, ETSIA, Universidad de Sevilla, Ctra Utrera Km 1, 41013 Sevilla, Spain; rperianez@us.es
* Correspondence: ccortes@us.es; Tel.: +34-954-486-483

Abstract

Accidental releases of radionuclides from nuclear-powered vessels or ships carrying nuclear weapons may expose marine organisms to radioactive contaminants. The consequences of such events can differ markedly between resident fish populations and migratory species that move through affected areas. While these contrasting responses have been evaluated by the authors for coastal nuclear accidents, comparable assessments for open-sea scenarios remain limited. We simulated radionuclide releases from vessels in the North Atlantic to evaluate exposure pathways and potential ecological effects on both resident and migratory fish, since several naval bases operating nuclear-powered vessels are located along the eastern North American coastline. Physical transport of radionuclides was modeled using a Lagrangian framework that incorporates advection by ocean currents, three-dimensional turbulent diffusion, radioactive decay, and dynamic sediment–water exchanges. This transport model was coupled to a four-compartment food-web bioaccumulation model representing phytoplankton, zooplankton, non-piscivorous fish, and piscivorous fish. The approach allows evaluation of contaminant uptake in resident fish populations and along the migration routes of highly mobile species. Bluefin tuna (*Thunnus thynnus*), a key ecological and commercially valuable species, was selected as the migratory case study. Migration paths reconstructed from electronic tagging data were integrated to estimate radionuclide exposure along individual trajectories. This combined modeling framework provides new insight into how open-sea nuclear releases may differentially affect resident fish communities and wide-ranging migratory species in the North Atlantic, with relevance for fish ecology, population risk assessment, and fisheries management.

Keywords: Lagrangian model; radionuclide transport; food-web model; bluefin tuna; caesium-137

Key Contribution: This study provides the first quantitative assessment of the contrasting effects of a hypothetical open-sea nuclear release on resident and migratory fish in the North Atlantic. By integrating radionuclide transport, food-web bioaccumulation, and electronic tagging data, it demonstrates that Atlantic bluefin tuna accumulate substantially lower levels of ^{137}Cs than resident fish, highlighting the importance of incorporating realistic migration behavior into marine radioecological risk assessments.

Academic Editor: Xinjun Chen

Received: 9 June 2026
Revised: 30 July 2026
Accepted: 4 August 2026
Published: 10 August 2026

1. Introduction

A number of numerical modeling studies have been published to assess the consequences of a hypothetical nuclear accident occurring in a land facility, such as a coastal nuclear power plant (NPP), in the marine environment. These are the cases of the Persian Gulf [1,2], the Korean Peninsula [3], the western and eastern Mediterranean Sea [4,5] respectively, the northeastern Atlantic Ocean [6], the Black Sea [7] and China seas [8], as some examples.

In addition to these works, numerical models have also been used to evaluate the radioactivity dispersion resulting from an accident in a nuclear-powered vessel or in a ship carrying nuclear weapons. Some of these models were applied to real nuclear accidents, such as the K-431 submarine in the Japan Sea [9]. The application of some models to this accident is also reviewed in [10]. Nevertheless, most model applications to simulate marine radionuclide dispersion after a nuclear accident on a ship deal with hypothetical accidents. These are the cases of [11] in the eastern Mediterranean, where an accident similar to that of the K-431 was simulated, and [12,13] in the Japan Sea, based on an accident similar to that of the Kursk submarine. An accident occurring after a potential recovery of the K-27 submarine, dumped in the Kara Sea, was simulated in [14,15]. Some hypothetical accidents occurring at different points along the transportation route of the submarine were assumed in these works. The transport of ^{137}Cs in the Barents Sea resulting from a hypothetical accident due to a self-sustained chain reaction in the reactors on the sunken nuclear submarine B-159 was analyzed in [16]. ^{137}Cs dispersion from the nuclear submarines Komsomolets and K-159 (renamed as B-159 in 1989), which are sunk in the Norwegian and Barents Seas, respectively, was simulated using realistic release rates under hypothetical scenarios by [17]. More recently, [18] simulated a hypothetical ^{3}H release from a nuclear-powered vessel in a port in the Yellow Sea. A summary of the main characteristics of these simulated accidents is presented in Table 1.

All these works present the common point that interactions of radionuclides between water and sediments are not considered, thus all radionuclides remain dissolved. In addition, the adsorption of radionuclide by biota is calculated only in [17], where a model based on a concentration factor, i.e., assuming that biota is in instantaneous equilibrium with water, is used. Instead, hypothetical accidents in submarines in the Kara Sea were simulated in [19], where ^{137}Cs and ^{60}Co releases were considered, including interactions of radionuclides with sediments. These processes are also considered in [2,4,6]. The transfer of radionuclides to biota, using a dynamic food-web model included within the radionuclide transport model, has been assessed in [1,6,20], where hypothetical accidents in land-based nuclear facilities in the Persian Gulf, the western Atlantic Ocean and the western Mediterranean, respectively, were simulated.

The consequences of such nuclear accidents can differ markedly between resident fish populations and migratory species that move through affected areas. While these contrasting responses have been evaluated by the authors for coastal nuclear accidents [6,21], comparable assessments for open-sea scenarios have not been carried out. The relevance of such open-sea scenarios has grown in recent decades alongside the expansion of nuclear-powered naval fleets and the increasing geopolitical attention to sunken or abandoned nuclear vessels. The potential for radionuclide releases from these sources, whether through structural deterioration or accidental events during recovery operations, underscores the need for predictive modeling frameworks capable of assessing ecological consequences across both resident and highly mobile marine species.

Table 1. Summary of simulated accidents in nuclear vessels in literature. RN: Radionuclide, Rel: release magnitude, Dur: release duration. NP: Information not provided in the paper. IR: Instantaneous release. CR: Continuous release. PT: Passive tracer (remains dissolved, no radionuclide specified).

Ref.	Area	RN	Rel. (Bq)	Dur.	Comment
[11]	East Mediterranean	^{137}Cs ^{90}Sr	2.2×10^8 2.7×10^8	10 days	Hypothetical accident similar to K-431 submarine accident; release to atmosphere and subsequent doses to marine biota are calculated.
[9]	Japan Sea	^{137}Cs ^{90}Sr ^{60}Co	4.4×10^9 4.1×10^9 1.2×10^{13}	NP	K-431 submarine accident; only qualitative assessment of marine dispersion. Half of releases to atmosphere and ocean.
[12]	Japan Sea	^{137}Cs	6.5×10^{15}	1 year	Hypothetical accident at distance to the coast (100 km) and depth (100 m) similar to Kursk submarine sinking.
[14]	Barents Sea	PT	NP	IR/CR	Hypothetical accident during recovery of dumped K-27 at different locations along its route. Continuous releases of 6 months, 1.5 and 10 years; surface and 300 m depth releases. Only qualitative results on dispersion patterns.
[15]	Barents Sea	^{137}Cs	1 PBq/0.4 PBq	IR	Hypothetical accident during recovery of dumped K-27; at different locations along route. The two releases correspond to maximum and realistic values.
[13]	Japan Sea	^{137}Cs	1.0×10^{12}	IR	Accident in hypothetical submarine similar to Kursk; surface release.
[16]	Barents Sea	^{137}Cs	5.0×10^{13}	IR	Sunk B-159 submarine; 6 month simulations; surface and sea bottom releases. Summer and winter release transport patterns are compared.
[17]	Norwegian Sea Barents Sea	^{137}Cs ^{137}Cs	3.1×10^{15}/500 GBq/y 5.2×10^{15}/500 GBq/y	IR/CR IR/CR	Kommosolets submarine. CR duration is 5 years; simulation time 5 years. K-159 submarine. CR duration is 5 year; simulation time 5 year.
[10]	Japan Sea	^{137}Cs	2.3×10^7	NP	K-431 accident; presents a summary of modeling studies for this accident.
[18]	Yellow Sea	^{3}H	1.5×10^{10} Bq/h	5 days	Hypothetical accident in a vessel in a port; results after 2 weeks of simulation.

The purpose of this paper is to simulate radionuclide releases from a vessel located in the open North Atlantic to evaluate potential ecological effects on both resident and migratory fish. The target radionuclide selected for this study is ^{137}Cs because it is chemically similar to potassium and accumulates in the fish flesh [22]. Atlantic bluefin tuna (*Thunnus thynnus*) was selected for the investigation as the migratory case study due to its high ecological and socioeconomic importance and its highly migratory behavior. A Lagrangian radionuclide transport model, including advection by currents, three-dimensional diffusion, radioactive decay and interactions with sediments, was used. Water–sediment interactions are described using a dynamic model with a single reversible reaction governed by kinetic transfer coefficients. Water currents, responsible for advective transport, are obtained from a global ocean circulation model, as described later. The Lagrangian model contains a dynamic food-web model with four compartments: phytoplankton, zooplankton, non-piscivorous fish, and piscivorous fish. Migration paths reconstructed from electronic tagging data were integrated to estimate radionuclide exposure along individual trajectories. Hypothetical accidents, with realistic ^{137}Cs source terms, are simulated, and resulting concentrations for resident and migratory fish are compared.

The methodology applied in this study is described in Section 2. Examples of results are presented in Section 3.

2. Methods

Only a brief overview of the mathematical model is provided in Section 2.1, since a detailed description and the corresponding equations can be found in [6] and the references therein. Next, actual tuna tracks for the migratory fish case are presented in Section 2.2 and numerical experiments in Section 2.3.

2.1. Mathematical Model

The modeling framework applied here combines a Lagrangian transport scheme with a food-web component. Radionuclide releases are represented by a collection of particles whose trajectories are tracked through time, each particle carrying an activity in Bq. The Lagrangian scheme accounts for advection by three-dimensional current fields, turbulent mixing in three dimensions, radioactive decay, and kinetic exchange reactions between dissolved radionuclides and seabed sediments. The model is formulated in spherical coordinates, as detailed in [4] and the references therein. Mixing, decay and water–sediment interactions are solved numerically using a stochastic (Monte Carlo) method.

The food-web component, embedded within the Lagrangian framework, resolves four trophic levels: phytoplankton, zooplankton, non-piscivorous fish, and piscivorous fish. At each level, radionuclide accumulation occurs through direct uptake from the water column and through ingestion of the preceding trophic level, while elimination is governed by a level-specific biological half-life. A full description of this model can be found in [1,20,22] among others.

An extension introduced in [21] and later used in [6] incorporates the migratory behavior of predatory fish into the framework. Specifically, the equation governing radionuclide concentration in tuna flesh (in the level of piscivorous fish) is evaluated at the fish's daily geographic position, so that uptake from both the water column and prey (non-piscivorous fish) reflects the local radionuclide concentrations at each successive location along the track, provided on a daily basis.

Ocean currents are responsible for advective transport. These data were obtained from the HYCOM (HYbrid Coordinate Ocean Model) global ocean model [23] for a domain spanning longitudes from $-82°$ to $-62°$ and latitudes from $25°$ to $47°$ (Figure 1). Horizontal resolution of this model is $0.08°$ in latitude and longitude, with 32 vertical levels increasing their thicknesses from the ocean surface to the bottom. HYCOM has been applied in the past to several problems in the North Atlantic Ocean, as in [24–26]. The transport simulations were driven by daily current fields, which are recycled on an annual basis when simulation periods exceed 365 days, following the approach described in [21] and also used in [6]. The surface velocity field for January 31st, depicted in Figure 1 as an example, illustrates the dominant circulation features of the region. The Gulf Stream appears as a well-defined northward jet along the continental margin, veering eastward into the open ocean at approximately 36° N, where it generates a rich field of meanders and mesoscale eddies [27]. This behavior is representative of the broader dynamical character of the western North Atlantic, whose circulation is shaped by the Gulf Stream system and its associated mesoscale activity. The current originates from the merger of the Florida Current and the Antilles Current, tracking northward along the continental slope until it separates from the coastline near Cape Hatteras (∼36° N) and enters the open ocean [28,29]. Beyond this separation point, the flow evolves into a sequence of meanders, warm-core rings, and cold-core eddies that facilitate exchange between subtropical and subpolar water masses across the frontal boundary [30].

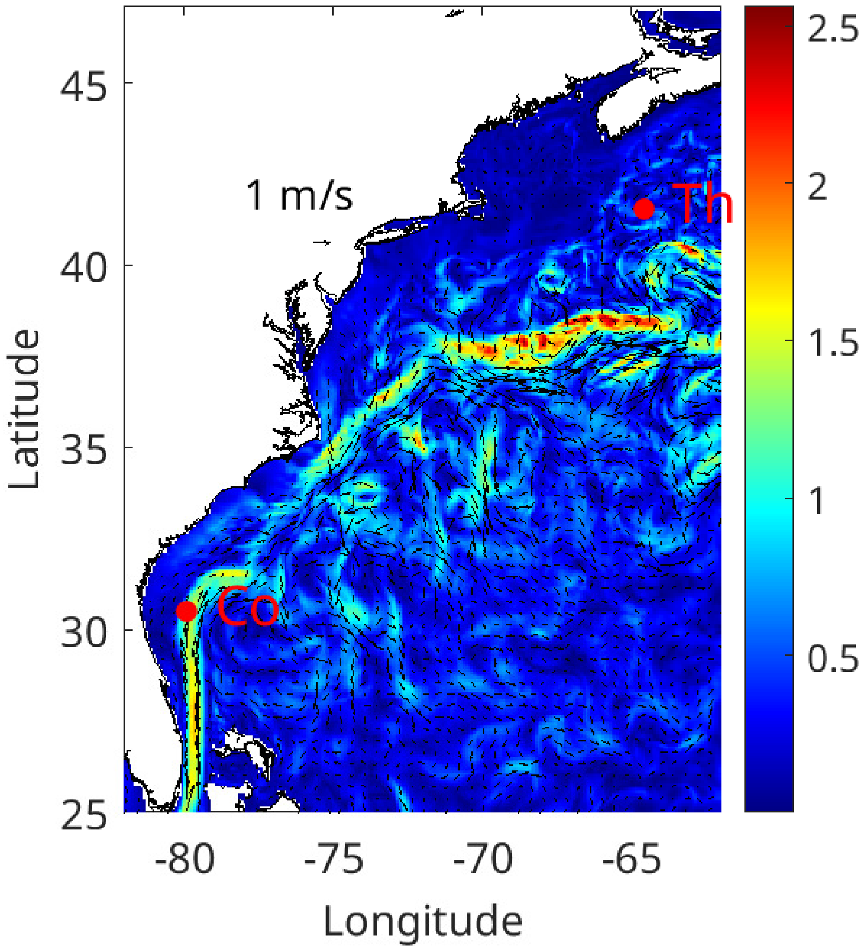

Figure 1. Model domain and surface circulation in January 31st, as an example. Only one in 25 current vectors is shown. The color scale provides the magnitude of the current in m/s. The red dots indicate the locations of the simulated accidents (Table 2).

Details of all model parameters and the justification for their values have been presented previously [6,21]; therefore, they are not repeated here. This model has already been applied to the North Atlantic and fully described in [6]; the same configuration is used in the present study.

Due to the hypothetical nature of the simulated accident scenarios, direct validation against measured ^{137}Cs concentrations in seawater, sediments, or tuna tissue is not possible. Nevertheless, confidence in the model results can be justified on several grounds. Provided that the underlying ocean circulation model reproduces observed current patterns adequately—something that can be independently verified against hydrographic data—the numerical methods employed for radionuclide transport are well-established and have been extensively evaluated. The Lagrangian model in particular has participated in formal intercomparison exercises coordinated by the International Atomic Energy Agency [31,32], where it performed successfully. The biota component was validated separately through comparisons with post-Fukushima field measurements of radionuclide concentrations in marine organisms [33], while the robustness of the tuna uptake submodel is assessed in [21] and illustrated in Figure 6 of that work.

Table 2. Numerical experiments. In the Exp column, Th-X and Co-X refers, respectively, to accidents in the Thresher location and in the coastal location; X is the tuna number. FTD is the date when the tuna enters the domain, which is the same as the simulated accident date, ST is the simulation time (in days) and Max *C* is the maximum calculated concentration in the tuna flesh (Bq/kg wet weight) for such an experiment (see Section 3 for discussion).

Exp	FTD	ST (d)	Max *C* (Bq/kg)
Th-1	19 May 1999	314	0.026
Th-4	27 May 2003	140	0.33
Th-15	30 March 1999	236	0.78
Co-5	5 January 2005	104	0.059
Co-7	2 November 2011	148	0.069
Co-14	1 November 2018	152	0.10
Co-15A	17 November 1997	149	0.058
Co-15B	21 November 1999	119	0.17

2.2. Tuna Tracks

The tuna tracks used in this study were obtained from tagging campaigns described by [34], conducted off the coasts of the United States and Canada by Stanford University; full methodological details are provided in that reference and the works cited therein. Where daily positional data were missing, linear interpolation between known locations was applied to maintain a continuous daily record, following the procedure of [6,21].

Depth records were available alongside the geographic coordinates for each daily position. As the tracked individuals spent most of their time at depths shallower than 50 m, radionuclide uptake from the water column was estimated using the mean concentration computed for the surface ocean layer at each daily location, consistent with the approach adopted in our previous works [6,21].

The distribution and movement of Atlantic bluefin tuna are closely tied to oceanographic conditions, particularly sea surface temperature and mesoscale circulation features. There is evidence that adult Atlantic bluefin tuna undertake seasonal migrations toward areas combining suitable thermal conditions and prey abundance [35,36], and that their vertical habitat use is thermally constrained, with individuals typically found in the uppermost 20 m during nighttime hours [37]. The northwestern Atlantic indeed functions as an important foraging ground for this species [34,38,39], where individuals concentrate for extended periods.

Not all of the available tuna tracks (15 in total) were used in the simulations. To represent conservative worst-case exposure scenarios, only individuals spending at least 90 days within a circular area of 300 km radius were selected. For the open-sea (Thresher) accident, this area was centered on the release location, due to the relatively small currents in this region, ensuring prolonged overlap between the fish and the radionuclide plume. For the coastal accident, however, the release point itself was not used because the Gulf Stream rapidly transports the radionuclide plume toward the northeast. Instead, the selection area was centered approximately 300 km northeast of the release location, corresponding to the trajectory of the contaminant plume and the region where tuna tend to remain for extended periods. This criterion maximizes the potential exposure of the selected individuals while remaining consistent with the worst-case philosophy adopted throughout the study, as was also done in previous studies [6,21]. Selected tuna tracks for the experiments described in Section 2.3 are plotted in Figure 2.

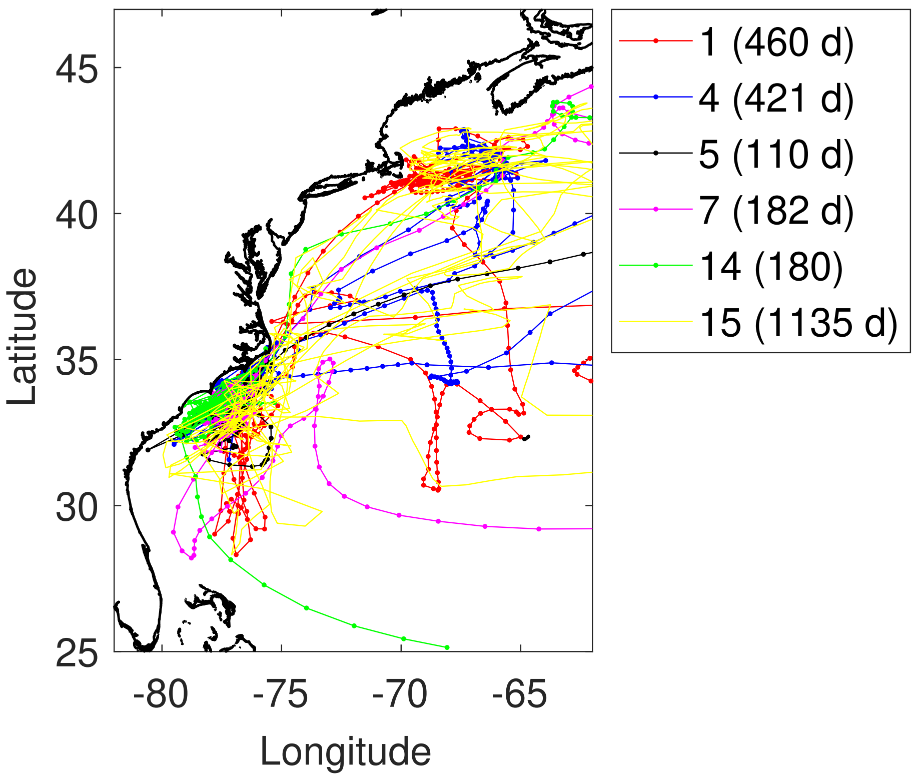

Figure 2. Daily positions, indicated as dots, of the selected tuna. The duration of the track in days is given in parenthesis.

2.3. Numerical Experiments

Using Table 1 as a reference of previously simulated nuclear accidents in vessels, the simulation conditions were established adopting a worst-case scenario. Thus, a ^{137}Cs release of 1 PBq has been assumed. Two types of accidents have been considered: an open-sea case in which there is an instantaneous release of all the activity at the surface and a case similar to that of [12], which considered an accident similar to the Kursk submarine, occurring close to the coast (some 100 km) and at a depth of 40 m.

The open-sea location was fixed as 41°46′ N, 65°3′ W, which is the location where the Thresher submarine sank in April 1963 (Figure 1). In this case, it was assumed that the entire release occurred instantaneously at the surface to deal with the worst case: as shown by [17], the highest concentration levels occur for rapid releases. In addition, a deep release (the submarine collapsed at 600 m depth and rests at 2600 m [40]) does not have a noticeable effect at the sea surface [41].

For the coastal accident, following [12] as mentioned above, the location 30°43′ N, 80°23′ W was fixed. This point is about 100 km from the coast; water depth is 50 m, and it is located in front of the Kings Bay Submarine Base, which is the U.S. Atlantic Fleet's home port for U.S. Navy Fleet ballistic missile nuclear submarines. In this case, the release was assumed to occur 10 m above the seabed (representing a sunken vessel), and to be instantaneous, representing a worst-case scenario. All experiments are summarized in Table 2. Experiments Th represent accident scenarios at the Thresher location (open sea), whereas Co corresponds to the coastal accident case. It should be clarified that tuna 15A and 15B from the Co experiments are the same tuna. This fish, numbered 15, exhibits two extended periods in the vicinity of the coastal accident location, separated by an interval of several months during which the tuna moves outside the model domain. For this reason, interpolating positions between both periods was deemed inappropriate, and each period near the accident site was instead treated as a separate tuna, as was already done in [6].

Since we are always dealing with worst-case scenarios, the date of the accident was systematically fixed as the date when the selected tuna entered the domain. It should be noted that this choice constitutes a deliberate worst-case assumption: by maximizing the temporal overlap between the tuna's presence in the domain and the radionuclide patch, the resulting flesh concentrations represent an upper bound on exposure for each individual track. Under realistic conditions, the probability of such an exact coincidence between an accidental release and the arrival of a migratory individual is inherently low, which further reinforces the conservative nature of the estimates presented here.

3. Results

The calculated concentrations of ^{137}Cs in water for the experiment Th-15 are shown in Figure 3 as an example for three specific days during the simulation. The instantaneous location of the tuna each day is also shown in the maps. Similarly, Figure 4 presents the corresponding concentrations calculated in non-piscivorous fish (food for tuna). First, it can be observed that a cyclonic circulation is apparent in the accident area, since the radionuclide patch travels toward the coast. This circulation is bounded at the south by the Gulf Stream (Figure 1). Although the release point is relatively close to the model boundary, water circulation in the area causes the radioactive patch to travel toward the inner domain. In addition, comparing both figures, it can be observed that the area affected by ^{137}Cs is larger in the case of non-piscivorous fish than in water. This is an expected result since, once the water becomes contaminated, some ^{137}Cs is taken up by the fish, which retain radionuclides due to the slow elimination rate, even after the affected water has been flushed away by currents.

Figure 5 provides temporal profiles of ^{137}Cs activity concentrations in tuna flesh, food, water and sediment for each daily location of the tuna. After 16 days, the ^{137}Cs concentration in the flesh starts to build up (although with very low values) as the fish takes up radionuclides from water and food. Later, there are more abrupt increases in the tuna concentrations (days 40 and 60) as the fish feed on more contaminated food. Afterward, there is a slow elimination of ^{137}Cs from tuna as it leaves the contaminated area. The maximum ^{137}Cs concentration in tuna flesh is in the order of 1 Bq/kg. Although the tuna travels over very contaminated water patches (days 20 and 90 approximately) and also may consume contaminated prey while passing through these regions, its transit time is too short to result in a substantial accumulation of ^{137}Cs in its flesh. It can also be seen in Figure 5 that there are four transits of the tuna over contaminated sediments, which, due to the dynamic nature of the water–sediment interaction model, may be acting as a source of radionuclides to the water column. However, this does not have a noticeable effect on the tuna flesh ^{137}Cs concentration.

The resulting ^{137}Cs concentration in piscivorous fish, calculated in the traditional way (considering static resident fish), can be seen in Figure 6. Maximum concentrations are in the order of 30 Bq/kg, which essentially is a factor of 10^2 larger than background in pelagic piscivorous fish (reported above) and a factor of 30 larger than the maximum concentration calculated in the migrating tuna (Figure 5). Figure 6 also shows the calculated concentration in bed sediments. It can be observed that deep-sea sediments are not reached by the radionuclides; only part of the continental shelf is contaminated, although levels are as high as 10^4 Bq/kg, which are even higher than those detected off Japan after the Fukushima accident [42]. In spite of vertical mixing, radionuclides do not reach the seabed in the area of the accident (water depth here is 2600 m and the release occurs at the surface). This is a logical result since the pycnocline acts as a natural barrier for vertical mixing and, in addition, vertical mixing in the ocean is much weaker than horizontal mixing (vertical mixing coefficients are orders of magnitude smaller than the horizontal ones) because of the very different turbulence scales in the horizontal and vertical directions of the ocean.

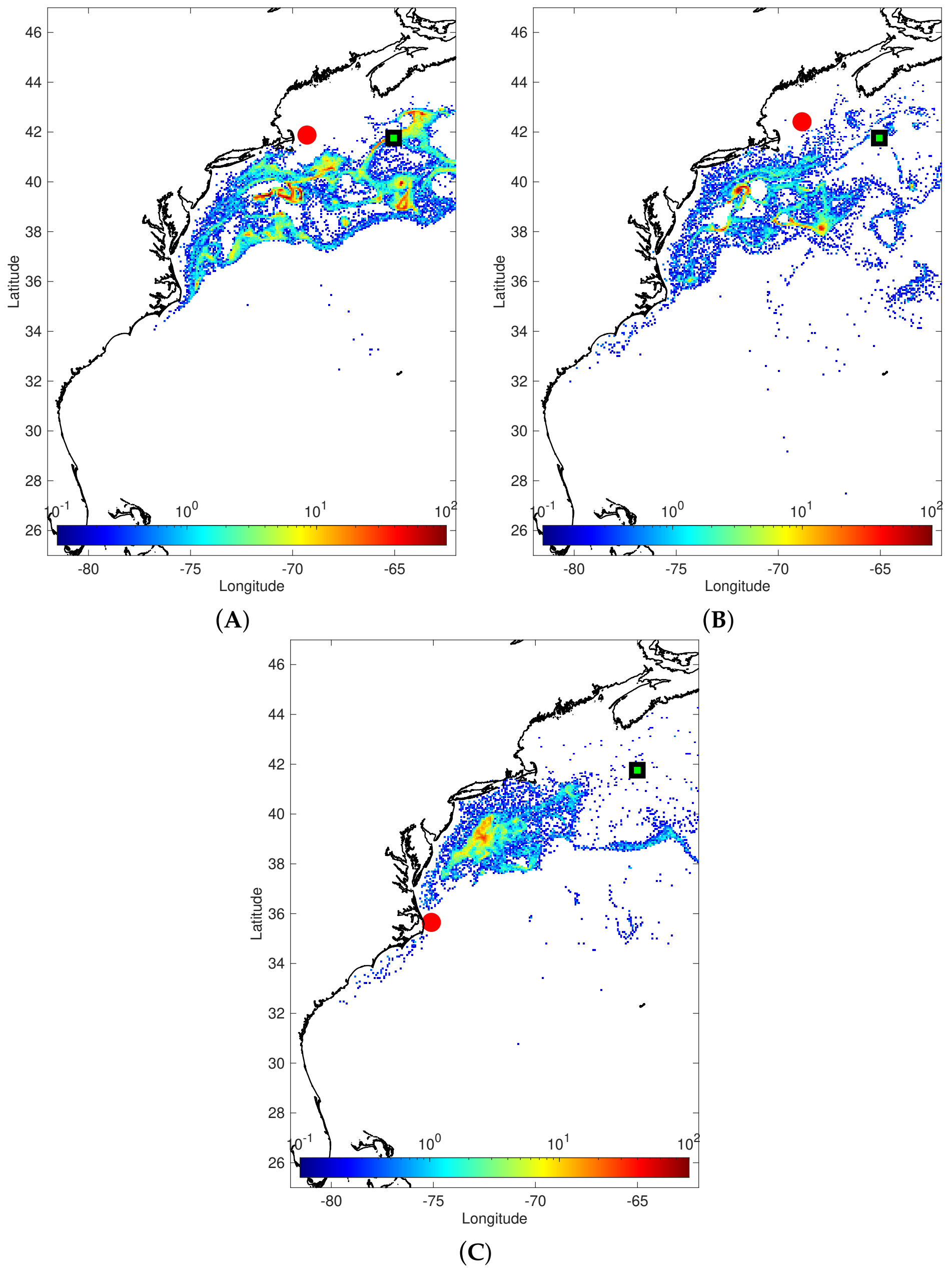

Figure 3. Maps of ^{137}Cs concentrations (Bq/m^3) in surface water for accident Th-15 in Table 2. Maps are drawn 120 (**A**), 180 (**B**) and 235 (**C**) days after the accident. The red dot marks the position of the tuna. The location of the accident is indicated by the black square filled in green.

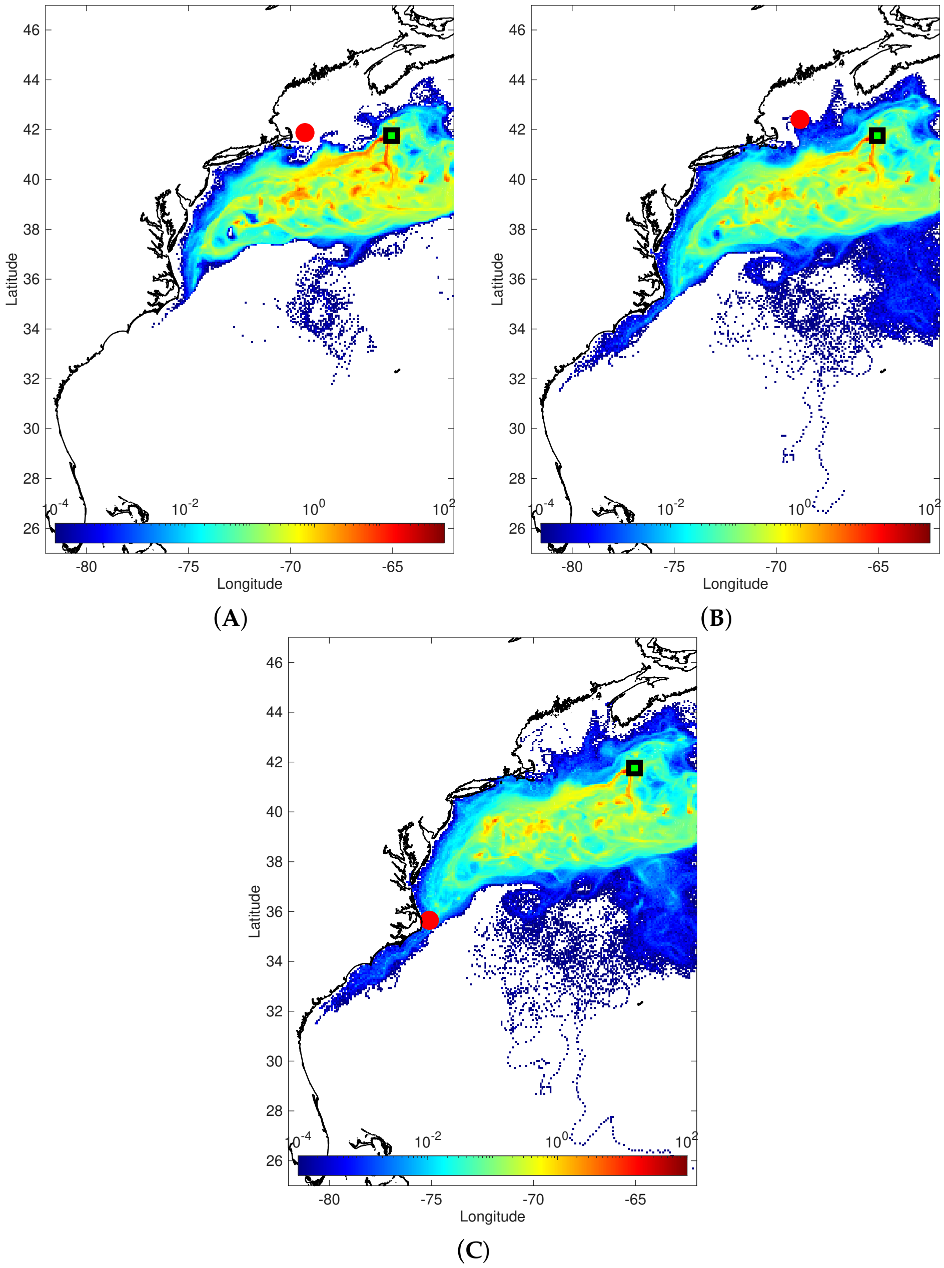

Figure 4. Maps of ^{137}Cs concentrations (Bq/kg ww) in non-piscivorous fish for accident Th-15 in Table 2. Maps are drawn 120 (**A**), 180 (**B**) and 235 (**C**) days after the accident. The red dot marks the position of the tuna. The location of the accident is indicated by the black square filled in green.

As shown in Table 2, which reports the maximum ^{137}Cs concentrations calculated in tuna flesh, none of the accidents occurring at the open-sea location have any effect on tuna. It should be noted that calculated concentrations in water and static resident fish (both piscivorous and non-piscivorous) for the other experiments are similar to those of experiment Th-15 since they are affected by differences in water circulation (due to different accident dates), but the release magnitude is the same and consequently maximum concentrations are in the same order. This is why we have chosen not to present these results here. The concentrations reported in Table 2 correspond to the deliberately selected worst-case exposure scenarios described in Section 2.

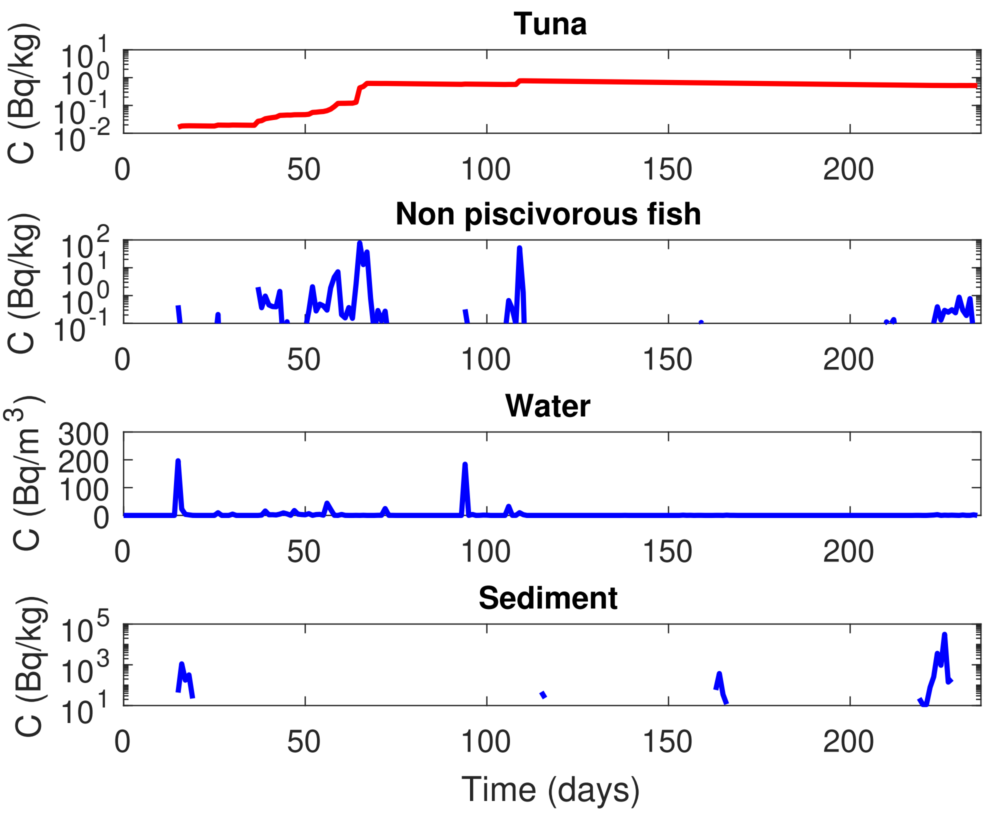

Figure 5. Time series of ^{137}Cs concentrations in the tuna flesh, non-piscivorous fish, water and sediment on each daily location of tuna for the experiment Th-15 in Table 2. Day number one corresponds to the accident date, which is when the tuna enters the domain (FTD in Table 2).

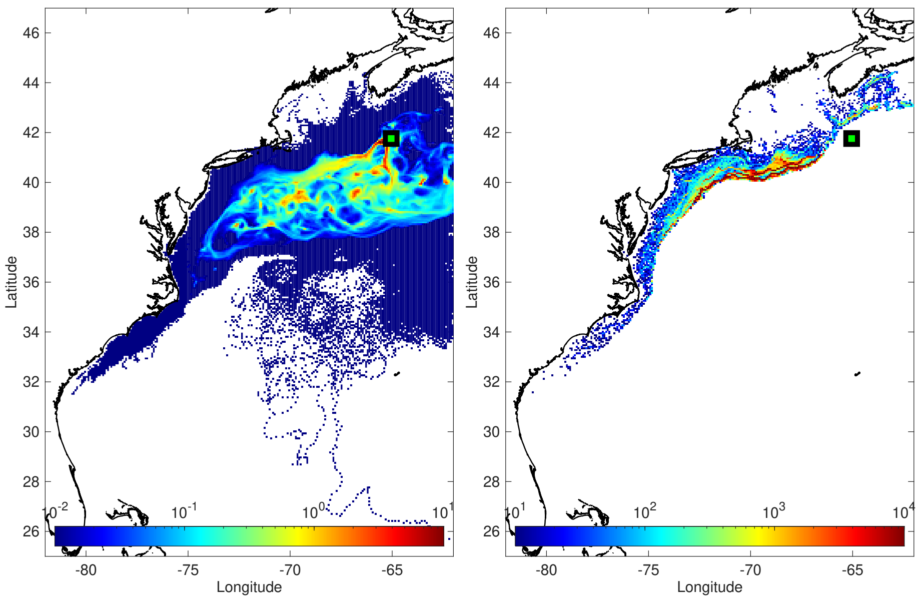

Figure 6. Maps of ^{137}Cs concentrations in piscivorous fish (**left**, Bq/kg) and sediments (**right**, Bq/kg) for accident Th-15 in Table 2 at the end of the simulation time. The location of the accident is indicated by the black square filled in green.

In the case of the coastal site accidents, it can be observed in Table 2 that maximum calculated ^{137}Cs concentrations in tuna flesh are of the same order of magnitude as in Th-experiments. Results for experiment Co-14 are presented as an example. The calculated concentrations in water and non-piscivorous fish at three specific days after the accident can be seen, respectively, in Figures 7 and 8. It is interesting to note that there is a plume of contaminated water extending to the northeast due to the Gulf Stream. Later, radionuclides are transported southward with meanders and gyres. In spite of being an instantaneous release, the plume expands from the release point and a concentration peak is clearly observed a few kilometers northeast of the accident location. This is due to the role of sediments, acting as a delayed source of radionuclides. Since the release occurs close to the seabed, bed sediments become heavily contaminated; these radionuclides are slowly redissolved and therefore the sediments behave as a long-term delayed source.

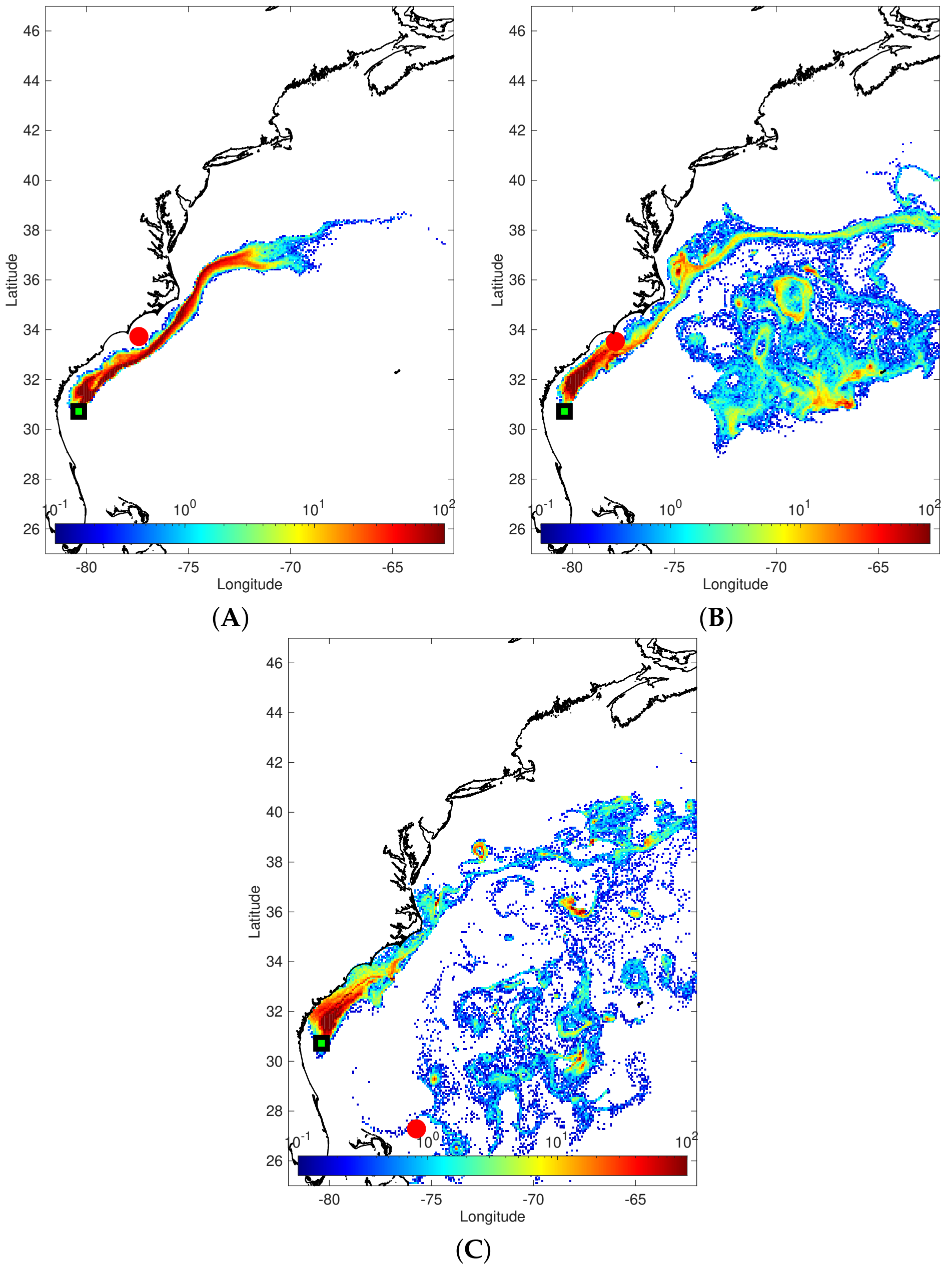

Figure 7. Maps of ^{137}Cs concentrations (Bq/m^3) in surface water for accident Co-14 in Table 2. Maps are drawn 50 (**A**), 100 (**B**) and 150 (**C**) days after the accident. The red dot marks the position of the tuna. The location of the accident is indicated by the black square filled in green.

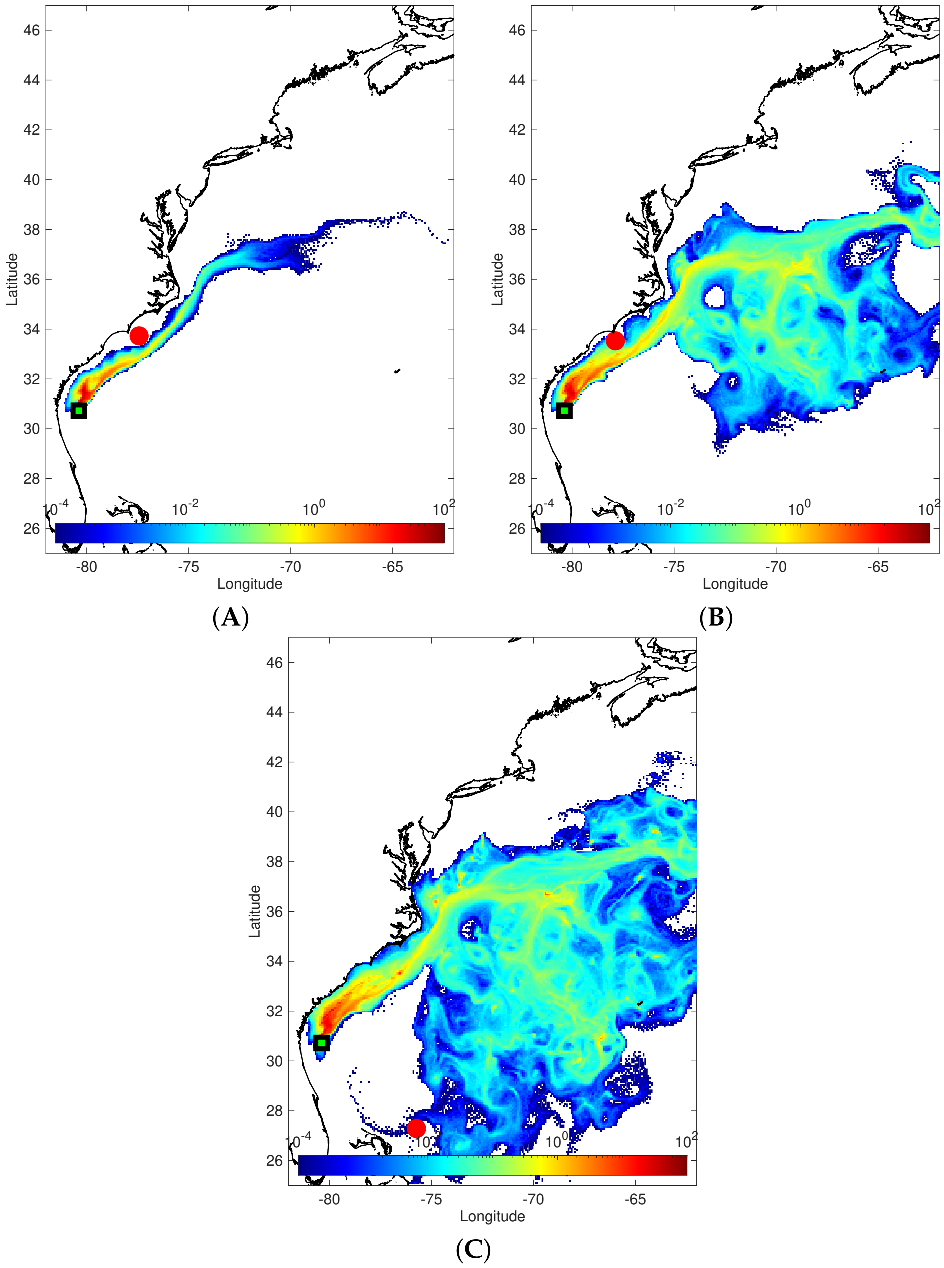

Figure 8. Maps of ^{137}Cs concentrations (Bq/kg ww) in non-piscivorous fish for accident Co-14 in Table 2. Maps are drawn 50 (**A**), 100 (**B**) and 150 (**C**) days after the accident. The red dot marks the position of the tuna. The location of the accident is indicated by the black square filled in green.

The temporal evolution of ^{137}Cs concentration in tuna flesh is presented in Figure 9, together with water, food and sediment along the tuna path. The tuna travels over areas with heavily contaminated sediments; however, the resulting concentrations in tuna flesh remain below 1 Bq/kg throughout the simulation.

Not surprisingly, the situation for resident piscivorous fish is different (Figure 10, left panel): ^{137}Cs concentrations reach 10^2 Bq/kg.

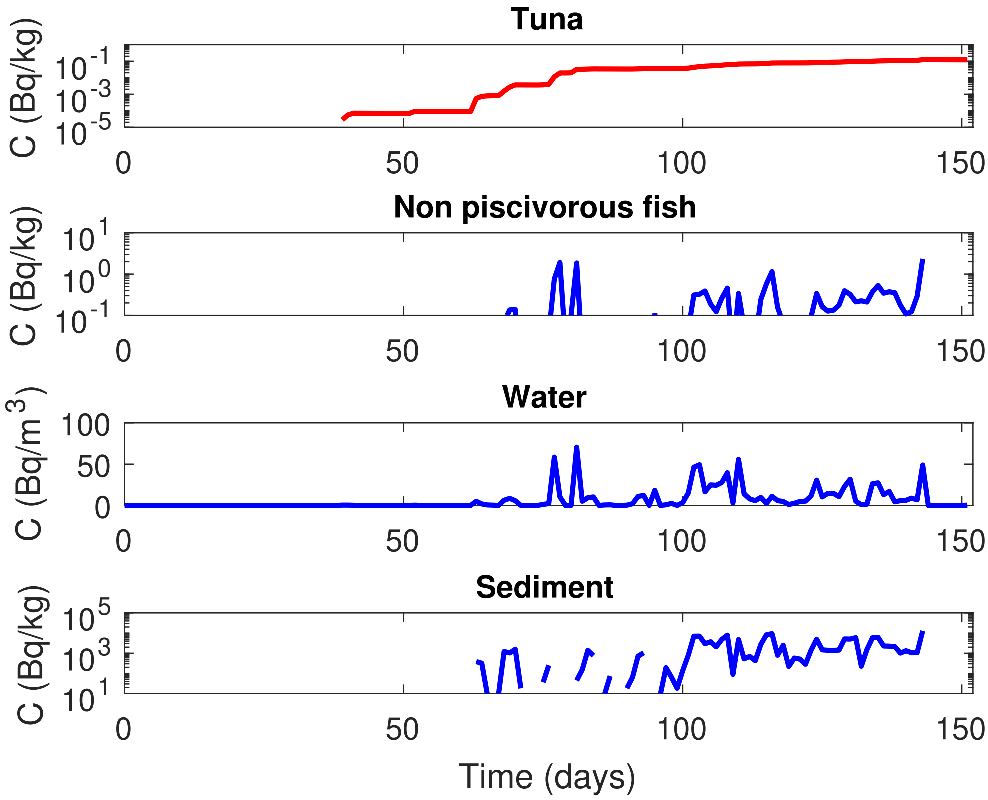

Figure 9. Time series of ^{137}Cs concentrations in the tuna flesh, non-piscivorous fish, water and sediment on each daily location of tuna for the experiment Co-14 in Table 2. Day number one corresponds to the accident date, which is when the tuna enters the domain (FTD in Table 2).

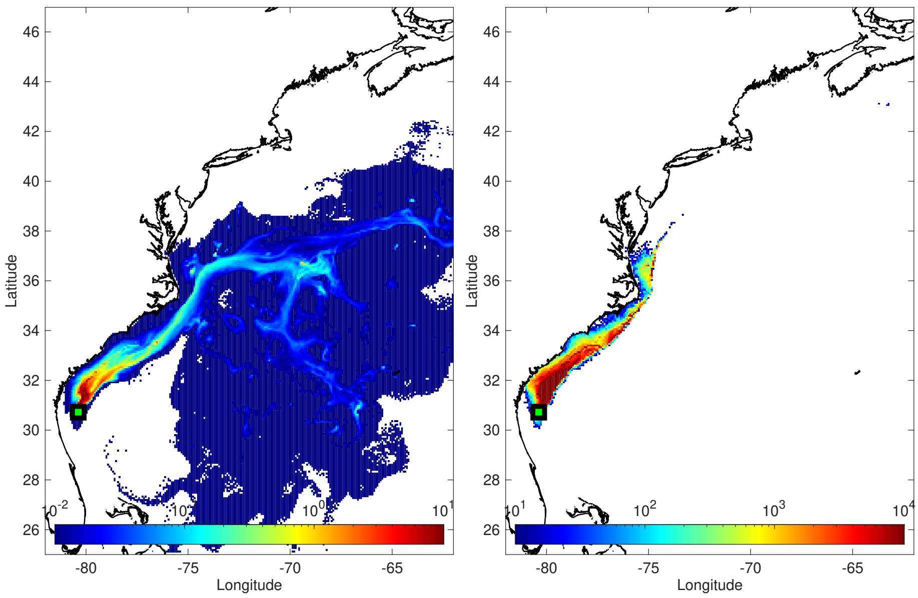

Figure 10. Maps of ^{137}Cs concentrations in piscivorous fish (**left**, Bq/kg) and sediments (**right**, Bq/kg) for accident Co-14 in Table 2 at the end of the simulation time. The location of the accident is indicated by the black square filled in green.

4. Discussion

4.1. Environmental Background Levels of ^{137}Cs

It is desirable to have some information on ^{137}Cs background levels in the different compartments considered in this work: water, sediment and fish. A typical ^{137}Cs background concentration in surface waters of the northern Atlantic Ocean is approximately

1.2 Bq/m^3 [43], a legacy of the atmospheric nuclear weapons tests conducted during the 1950s and 1960s. This value is comparable to the pre-Fukushima baseline documented for the northern Pacific Ocean, which ranged between 1 and 2 Bq/m^3 [44].

Background ^{137}Cs concentrations in non-piscivorous fish, drawn from the IAEA MARIS database [43], are on the order of 10^{-1} Bq/kg wet weight (WW) across several regions in the world ocean, including the Bay of Bengal, the North Sea, and the western Barents Sea. Somewhat lower levels have been reported in the Persian Gulf, where Uddin et al. [45] measured values of around 0.034 Bq/kg (WW). Along the US east coast, a concentration of 0.33 Bq/kg (WW) has been recorded off North Carolina, with broadly comparable levels observed in waters off Newfoundland [43].

Pelagic piscivorous fish from the Pacific Ocean generally exhibit ^{137}Cs concentrations below 10^{-1} Bq/kg, though levels as high as 10^3 Bq/kg were recorded in the vicinity of the Fukushima NPP in the aftermath of the March 2011 accident [46–48]. For bluefin tuna specifically, the review by Fakhri et al. [49] reports a global mean ^{137}Cs concentration in fish flesh of 0.42 Bq/kg dry weight (DW), which converts to approximately 0.10 Bq/kg wet weight (WW) following [50]. To ensure consistency with model output, all concentrations reported in this work are expressed on a wet weight basis, with dry weight values converted accordingly where necessary. Individual measurements contributing to this global mean span a range from 0.0083 to 0.40 Bq/kg [49]. A pre-Fukushima background of approximately 0.25 Bq/kg WW in Pacific bluefin tuna was reported in [51], in good agreement with the mean value in [49]. These background concentrations collectively serve as reference levels against which simulation results are assessed. Following the Fukushima accident, Madigan et al. [51] measured elevated ^{137}Cs concentrations (1.6 ± 0.4 Bq/kg) in bluefin tuna sampled off the US coast, while estimating that concentrations near the Japanese coast could have been 1.5 to 15 times higher, given the progressive elimination of ^{137}Cs during the transoceanic migration. Povinec and Hirose [52] reported a broader range of 0.3–41 Bq/kg for tuna caught in the open Pacific after the accident. With respect to the safety limit for ^{137}Cs concentration in tuna flesh information, which is also useful information, it was set by Japan to 100 Bq/kg [50] and the European Union fixed it as 1250 Bq/kg [53].

4.2. Comparison with Previous Observations and Modeling Studies

Resident non-piscivorous and piscivorous fish located within the contaminated area reach concentrations several orders of magnitude above natural background levels, reflecting their continuous exposure to contaminated water and prey. In contrast, the maximum concentration predicted for Atlantic bluefin tuna in the open-sea experiments is approximately 0.78 Bq kg/kg wet weight, while all coastal simulations produce concentrations of the same order of magnitude or lower. Although these values exceed typical environmental background concentrations reported for tuna, they remain within the lower range of concentrations measured after the Fukushima accident and are two to three orders of magnitude below internationally accepted food-safety limits.

The question of whether migratory fish accumulate radiologically significant levels of ^{137}Cs following a coastal nuclear accident was first addressed in a Northwest Mediterranean context in [21], where tuna tracks around a hypothetical accident near northeast Spain consistently yielded flesh concentrations below background, and later in the Northern Atlantic Ocean [6] with similar conclusions.

The simulated tuna concentrations are also broadly consistent with field observations reported after the Fukushima Daiichi accident. Measurements of Pacific bluefin tuna and other marine fish showed detectable increases in ^{137}Cs concentrations following the accident, although values generally remained well below internationally accepted food-safety limits. The maximum concentrations predicted in the present study fall within the lower range of those reported after Fukushima and therefore support the conclusion that, even under an intentionally conservative accident scenario, radiological impacts on migratory tuna would remain limited.

A much stronger response is predicted for resident fish inhabiting the contaminated area. Non-piscivorous fish reach concentrations of the order of 10^2 Bq kg/kg, while resident piscivorous fish accumulate approximately 30 Bq kg/kg, largely above background.

The present study addresses a scenario that differs substantially from those examined in previous work [6,21]: rather than a hypothetical accident at a coastal nuclear power plant, the release originates from a nuclear-powered vessel operating in the open North Atlantic Ocean. This distinction has important physical consequences for radionuclide dispersal. In the coastal NPP scenarios, the proximity of the source to the continental shelf promotes rapid sediment interaction and retains part of the contamination in nearshore waters. In the open-sea case simulated here, the released ^{137}Cs is subject to the full dilution capacity of the open ocean from the outset, with the dominant transport controlled by the large-scale circulation, notably the cyclonic gyre apparent in the accident area and the bounding influence of the Gulf Stream to the south (Figure 1).

4.3. Ecological Implications and Fish Mobility

A key result with broader methodological implications concerns the differences between migratory tuna and resident fish, as demonstrated through the comparisons with environmental background levels. The principal outcome of the simulations is not the absolute magnitude of radionuclide concentrations, but the marked contrast between resident and highly migratory species.

As shown in Figure 6, resident piscivorous fish near the accident location accumulate ^{137}Cs concentrations of the order of 30 Bq/kg—approximately 30 times higher than the maximum calculated for any of the tracked tuna, and two orders of magnitude above background. Non-piscivorous fish in the same area show concentrations reaching $\sim 10^2$ Bq/kg (Figures 4 and 5), largely exceeding background. This contrast reinforces the conclusion reached in previous studies [6,21] that models treating all fish as stationary residents substantially overestimate radionuclide uptake in migratory species, and highlights the importance of incorporating realistic movement behavior into radioecological risk assessments.

Previous studies have shown that radionuclide accumulation in fish is strongly influenced by trophic position, feeding ecology and metabolic characteristics [54], while radionuclide transfer through marine food webs depends on complex biokinetic and environmental processes [55]. In this context, the very low radionuclide concentrations predicted here for migratory tuna indicate that the associated ecological consequences are expected to be negligible, despite substantially higher contamination levels predicted for resident fish.

It is also worth noting that contaminated sediments are confined to the continental shelf and do not extend into the deep sea (Figure 6), though their dynamic re-release of radionuclides to the water column is captured by the kinetic interaction model. Bed sediments of the shelf become heavily contaminated; these radionuclides are slowly redissolved, and therefore the sediments behave as a long-term delayed source, an effect that has been observed in the Irish Sea after the releases from Sellafield nuclear fuel reprocessing plant [56]. This is confirmed in Figure 10, which shows calculated ^{137}Cs concentrations in sediments at the end of the simulation. Sediments of the shallow continental shelf are contaminated due to the transit of contaminated water above them and a considerable ^{137}Cs-contaminated patch, with concentrations reaching 10^5 Bq/kg evident. Then, these sediments gradually release radionuclides back into the water column.

4.4. Model Limitations

Several limitations of the present modeling framework should be acknowledged. First, the simulations were intentionally designed as worst-case scenarios by synchronizing the accidental release with the arrival of each selected tuna in the study domain. Consequently, the predicted radionuclide concentrations should be interpreted as conservative upper-bound estimates rather than as average exposure levels for the Atlantic bluefin tuna population. Second, zooplankton advection by the Gulf Stream is not explicitly represented, which may introduce some uncertainty into the trophic transfer pathway. Third, the available migration tracks represent only a subset of the behavioral diversity of Atlantic bluefin tuna, while additional uncertainties arise from the biological uptake parameters and the HYCOM-derived current fields used to drive radionuclide transport. Finally, the model considers only direct releases into the marine environment and does not include atmospheric releases followed by deposition onto the ocean surface, a process that could increase radionuclide exposure over broader regions and deserves future investigation. Nevertheless, none of these limitations is expected to alter the principal conclusion of this study, since the marked difference between migratory and resident fish is primarily controlled by exposure duration rather than by uncertainties in individual model parameters.

5. Conclusions

A Lagrangian radionuclide transport model coupled with a four-compartment dynamic food-web module has been applied to simulate ^{137}Cs dispersion and bioaccumulation following hypothetical nuclear accidents from a vessel in the North Atlantic Ocean. Two accident scenarios were considered: an open-sea release at the location of the USS Thresher submarine (41°46′ N, 65°3′ W), and a coastal release approximately 100 km offshore Kings Bay Submarine Base, Georgia, at 40 m depth. In both cases, an instantaneous worst-case release of 1 PBq was assumed. Water circulation was obtained from the HYCOM global ocean model, and migration paths of Atlantic bluefin tuna (*Thunnus thynnus*) derived from electronic tagging data were integrated into the model to estimate radionuclide exposure along individual trajectories.

For the open-sea accident scenario, ^{137}Cs concentrations accumulated in migratory Atlantic bluefin tuna remained low in all simulations, reaching a maximum value of approximately 0.78 Bq kg/1 wet weight in the most exposed individual. The results indicate that radionuclide accumulation is primarily controlled by the short residence time of tuna within contaminated water masses, which limits exposure despite the conservative 1 PBq instantaneous release considered in the simulations.

A marked contrast emerges when comparing migratory tuna with resident static fish. Resident piscivorous fish near the accident site accumulate ^{137}Cs concentrations of approximately 30 Bq/kg, roughly 30 times higher than the maximum calculated for any tracked tuna, and two orders of magnitude above background. Non-piscivorous fish reach concentrations of the order of 10^2 Bq/kg in the same area. These findings demonstrate that a realistic representation of fish movement is essential for reliable radioecological risk assessment of highly migratory marine species.

Contaminated sediments are confined to the continental shelf and do not penetrate into the deep sea, though the kinetic water–sediment interaction model captures their role as a secondary ^{137}Cs source to the overlying water column. The cyclonic circulation in the accident area, bounded to the south by the Gulf Stream, controls the large-scale dispersal pattern and drives the radionuclide patch progressively toward the coast over the simulation period.

https://doi.org/10.3390/fishes11080467

Results for the coastal accident scenario indicate that, given the location of the accident site over the continental shelf, stronger sediment interaction and higher local concentrations in water and resident biota are calculated compared to the open-sea case.

Overall, this study extends the evaluation of open-sea nuclear vessel accident consequences to both static and migratory fish populations in the North Atlantic, providing new quantitative estimates for a region of strategic and ecological relevance. The modeling framework developed here is transferable to other marine domains and contaminant scenarios, and contributes a decision-support tool for post-accident environmental assessment and fisheries management planning.

Author Contributions: Methodology, C.C. and R.P.; Software, C.C. and R.P.; Validation, C.C. and R.P.; Formal analysis, C.C. and R.P.; Investigation, C.C. and R.P.; Resources, C.C. and R.P.; Writing—review & editing, C.C. and R.P. All authors have read and agreed to the published version of the manuscript.

Funding: This research received no external funding.

Institutional Review Board Statement: Ethical review and approval were waived for this study because no animal experiments were conducted.

Data Availability Statement: The raw data supporting the conclusions of this article will be made available by the authors on request.

Conflicts of Interest: The authors declare no conflicts of interest.

References

1. Maderich, V.; Bezhenar, R.; Kovalets, I.; Khalchenkov, O.; Brovchenko, I. Long–Term Contamination of the Arabian Gulf as a Result of Hypothetical Nuclear Power Plant Accidents. *J. Mar. Sci. Eng.* **2023**, *11*, 331. [CrossRef]
2. Periáñez, R. APERTRACK: A particle-tracking model to simulate radionuclide transport in the Arabian/Persian Gulf. *Prog. Nucl. Energy* **2021**, *142*, 103998. [CrossRef]
3. Min, J.S.; Kim, H.R. Environmental impact on the Korean peninsula due to hypothetical accidental scenarios at the Haiyang nuclear power plant in China. *Progr. Nucl. Energy* **2018**, *105*, 254–262. [CrossRef]
4. Periáñez, R.; Cortés, C. A Numerical model to simulate the transport of radionuclides in the Western Mediterranean after a nuclear accident. *J. Mar. Sci. Eng.* **2023**, *11*, 169. [CrossRef]
5. Tsabaris, C.; Tsiaras, K.; Eleftheriou, G.; Triantafyllou, G. ^{137}Cs ocean distribution and fate at East Mediterranean Sea in case of a nuclear accident in Akkuyu Nuclear Power Plant. *Progr. Nucl. Energy* **2021**, *139*, 103879. [CrossRef]
6. Cortés, C.; Periáñez, R.; Block, B.A.; Castleton, M.R.; Cermeño, P.; Dedman, S. Modelling the accumulation of ^{137}Cs by Atlantic bluefin tuna (*Thunnus thynnus*) A Hypothetical Nucl. Accid. Northwest Atl. Ocean. *J. Mar. Syst.* **2026**, *253*, 104180. [CrossRef]
7. Bezhenar, R.; Kovalets, I. Modeling of radioactive contamination of the Black Sea and its impact on humans due to hypothetical heavy accident at the Zaporizhzhia NPP. In *Mathematical Modeling and Simulation of Systems. MODS 2022*; Shkarlet, S., Morozov, A., Palagin, A., Vinnikov, D., Stoianov, N., Zhelezniak, M., Kazymyr, V., Eds.; Lecture Notes in Networks and Systems; Springer: Berlin/Heidelberg, Germany, 2023; Volume 667.
8. Brovchenko, I.; Kim, K.O.; Maderich, V.; Jung, K.T.; Bezhenar, R.; Ryu, J.H.; Min, J.E. Sediment and radioactivity transport in the Bohai, Yellow, and east China seas: A modeling study. *J. Mar. Sci. Eng.* **2022**, *10*, 596. [CrossRef]
9. Budyansky, M.V.; Fayman, P.A.; Uleysky, M.Y.; Prants, S.W. The impact of circulation features on the dispersion of radionuclides after the nuclear submarine accident in Chazhma Bay (Japan Sea) in 1985: A retrospective Lagrangian simulation. *Mar. Pollut. Bull.* **2022**, *177*, 113483. [CrossRef] [PubMed]
10. Sarkisov, A.A.; Vysotskii, V.L. The largest nuclear accident in the history of the nuclear fleet. Reconstruction of events and analysis of the accident consequences to assess the risks and hazards of small nuclear power facilities. *Nucl. Eng. Des.* **2021**, *384*, 111440. [CrossRef]
11. Abbasi, A.; Mirekhtiary, F.; Khandaker, M.U.; Maden, S.; Ali, A.H. Radiological and ecological consequences of a hypothetical nuclear submarine accident in the Eastern Mediterranean. *J. Radioanal. Nucl. Chem.* **2025**, *334*, 6169–6177. [CrossRef]
12. Kobayashi, T.; Togawa, O.; Odano, N.; Ishida, T. Estimates of collective doses from a hypothetical accident of a nuclear submarine *J. Nucl. Sci. Technol.* **2001**, *38*, 658–663. [CrossRef]
13. Kobayashi, T.; Chino, M.; Togawa, O. Numerical simulations of short-term migration processes of dissolved cesium-137 due to a hypothetical accident of a nuclear submarine in the Japan Sea. *J. Nucl. Sci. Technol.* **2006**, *43*, 569–575. [CrossRef]

14. Karcher, M.; Hosseini, A.; Schnur, R.; Kauker, F.; Brown, J.E.; Dowdall, M.; Strand, P. Modelling dispersal of radioactive contaminants in Arctic waters as a result of potential recovery operations on the dumped submarine K-27. *Mar. Pollut. Bull.* **2017**, *116*, 385–394. [CrossRef] [PubMed]
15. Hosseini, A.; Amundsen, I.; Brown, J.; Dowdall, M.; Karcher, M.; Kauker, F.; Schnur, R. Impacts on the marine environment in the case of a hypothetical accident involving the recovery of the dumped Russian submarine K-27, based on dispersion of ^{137}Cs. *J. Environ. Radioact.* **2017**, *167*, 170–179. [CrossRef] [PubMed]
16. Antipov, S.W.; Bilashenko, V.P.; Vysotskii, V.L.; Kalantarov, V.E.; Kobrinskii, M.N.; Sarkisov, A.A.; Sotnikov, V.A.; Shvedov, P.A.; Ibraev, R.A.; Sarkisyan, A.S. Prediction and evaluation of the radioecological consequences of a hypothetical accident on the sunken nuclear submarine B-159 in the Barents Sea. *At. Energy* **2015**, *119*, 106–113. [CrossRef]
17. Heldal, H.E.; Vikebø, F.; Johansen, G.O. Dispersal of the radionuclide caesium-137 (^{137}Cs) from point sources in the Barents and Norwegian Seas and its potential contamination of the Arctic marine food chain: Coupling numerical ocean models with geographical fish distribution data. *Environ. Pollut.* **2013**, *180*, 190–198. [CrossRef] [PubMed]
18. Li, Z.; Chen, R.; Xing, X.; Liu, C.; Wang, Z.; Wang, N.; Wang, Z.; Xue, Q. Research on dispersion patterns and discharge control of radionuclides from nuclear-powered vessels. *Ann. Nucl. Energy* **2026**, *227B*, 111992. [CrossRef]
19. Periáñez, R. A numerical model to assess the consequences of a nuclear accident in the Kara Sea. *Reg. Stud. Mar. Sci.* **2025**, *92*, 104627. [CrossRef]
20. Periáñez, R.; Cortés, C. A study on the transport of ^{137}Cs and ^{90}Sr in marine biota in a hypothetical scenario of a nuclear accident in the western Mediterranean Sea. *J. Mar. Sci. Eng.* **2023**, *11*, 1707. [CrossRef]
21. Cortés, C.; Periáñez, R.; Block, B.A.; Castleton, M.R.; Cermeño, P.; Dedman, S. Numerical modelling of radionuclide uptake by bluefin tuna along its migration routes in the Mediterranean Sea after a nuclear accident. *Mar. Environ. Res.* **2024**, *202*, 106757. [CrossRef] [PubMed]
22. Maderich, V.; Jung, K.T.; Bezhenar, R.; de With, G.; Qiao, F.; Casacuberta, N.; Masque, P.; Kim, Y.H. Dispersion and fate of ^{90}Sr in the Northwestern Pacific and adjacent seas: Global fallout and the Fukushima Dai-ichi accident. *Sci. Total Environ.* **2014**, *494–495*, 261–271. [CrossRef] [PubMed]
23. Bleck, R. An oceanic general circulation model framed in hybrid isopycnic–Cartesian coordinates. *Ocean Model.* **2001**, *4*, 55–88.
24. Hofmann, E.E.; Druon, J.N.; Fennel, K.; Friedrichs, M.; Haidvogel, D.; Lee, C.; Mannino, A.; McClain, C.; Najjar, R.; Siewert, J.; et al. Eastern U.S. continental shelf carbon budget: Integrating models, data assimilation, and analysis. *Oceanography* **2008**, *21*, 86–104. [CrossRef]
25. Samuelsen, A.; Bertino, L.; Hansen, C. Impact of data assimilation of physical variables on the spring bloom from TOPAZ operational runs in the North Atlantic. *Ocean. Sci.* **2009**, *5*, 635–647. [CrossRef]
26. Timko, P.G.; Arbic, J.G.; Richman, R.B.; Scott, E.J.; Metzger, A.J.; Wallcraft, B.K. Skill tests of three-dimensional tidal currents in a global ocean model: A look at the North Atlantic. *J. Geophys. Res.* **2012**, *117*, C08014. [CrossRef]
27. Open University. *Ocean Circulation*; Butterworth-Heinemann: Oxford, UK, 2002.
28. Hogg, N.G.; Johns, W.E. Western boundary currents. *Rev. Geophys.* **1995**, *33*, 1311–1334. [CrossRef]
29. Bower, A.S.; Hunt, H.D. Lagrangian observations of the deep western boundary current in the North Atlantic Ocean. *Deep-Sea Res. I* **2000**, *47*, 37–61.
30. Richardson, P.L. Average velocity and transport of the Gulf Stream near 55° W. *J. Mar. Res.* **1985**, *43*, 83–111. [CrossRef]
31. IAEA. *Modelling of Marine Dispersion and Transfer of Radionuclides Accidentally Released from Land Based Facilities*; IAEA-TECDOC-1876; IAEA: Vienna, Austria, 2019.
32. IAEA. *Enhancement of Modelling Approaches for the Assessment of Radionuclide Transfer in the Marine Environment*; IAEATECDOC-2060; IAEA: Vienna, Austria, 2024.
33. Periáñez, R.; Bezhenar, R.; Brovchenko, I.; Jung, K.T.; Kamidara, Y.; Kim, K.O.; Kobayashi, T.; Liptak, L.; Maderich, V.; Min, B.I.; et al. Fukushima ^{137}Cs releases dispersion modelling over the Pacific Ocean. Comparisons of models with water, sediment and biota data. *J. Environ. Radioact.* **2019**, *198*, 50–63. [CrossRef] [PubMed]
34. Dedman, S.; Aalto, E.A.; Stokesbury, M.J.W.; Schallert, R.J.; Castleton, M.R.; Block, B.A. Assignment of tracks from tagged Atlantic bluefin tuna *Thunnus thynnus* Potential Stock Using Behavioural Differences and Habitat Partitioning. *Front. Mar. Sci.* **2023**, *10*, 1165910. [CrossRef]
35. Block, B.A.; Dewar, H.; Blackwell, S.B.; Williams, T.D.; Prince, E.D.; Farwell, C.J.; Weng, K.C.; Dewar, H.; Williams, T.D. Electronic tagging and population structure of Atlantic bluefin tuna. *Nature* **2005**, *434*, 1121–1127. [CrossRef] [PubMed]
36. Madin, E.M.P.; Madin, J.S. Predators, facilitators, or both? Re-evaluating an apparent predator-prey relationship. *Mar. Ecol. Prog. Ser.* **2011**, *431*, 299–302. [CrossRef]
37. Horton, W.H.; Binney, F.C.T.; Birch, S.; Block, B.A.; Exeter, O.M.; Garzon, F.; Plaster, A.; Righton, D.; van der Kooij, J.; Witt, M.J.; et al. Annual migrations, vertical habitat use and fidelity of Atlantic bluefin tuna tracked from waters off the United Kingdom. *Sci. Rep.* **2025**, *15*, 293. [CrossRef] [PubMed]

38. Cermeño, P.; Quílez-Badia, G.; Ospina-Alvarez, A.; Sainz-Trápaga, S.; Boustany, A.M.; Seitz, A.C.; Tudela, S.; Block, B.A. Electronic Tagging of Atlantic Bluefin Tuna (*Thunnus thynnus*, L.) Reveal. Habitat Use Behav. Mediterr. Sea. *PLoS ONE* **2015**, *10*, e0116638. [CrossRef] [PubMed]
39. Abascal, F.J.; De La Serna, A.; Medina, D.; Godoy, J.; Aranda, G. Tracking bluefin tuna reproductive migration into the Mediterranean Sea with electronic pop-up satellite archival tags using two tagging procedures. *Fish. Oceanogr.* **2016**, *25*, 54–66. [CrossRef]
40. Proceedings of the U.S. Naval Institute. What Killed the Thresher? 2023. Available online: https://www.usni.org/magazines/naval-history-magazine/2023/april/what-killed-thresher (accessed on 8 December 2025).
41. Periáñez, R.; Suh, K.S.; Min, B.I. The behaviour of ^{137}Cs in the North Atlantic Ocean assessed from numerical modelling: Releases from nuclear fuel reprocessing factories, redissolution from contaminated sediments and leakage from dumped nuclear wastes. *Mar. Pollut. Bull.* **2016**, *113*, 343–361. [CrossRef] [PubMed]
42. Suzuki, S.; Amano, A.; Enomoto, M.; Matsumoto, A.; Morioka, Y.; Sakuma, K.; Tsuruta, T.; Kaeriyama, H.; Miura, H.; Tsumune, D.; et al. Temporal variability of ^{137}Cs concentrations in coastal sediments off Fukushima. *Sci. Total Environ.* **2022**, *831*, 154670. [CrossRef] [PubMed]
43. IAEA, 2023. IAEA MARIS. Marine Radioactivity Information System, Division of IAEA Environment Laboratories: Monaco. Available online: https://maris.iaea.org (accessed on 4 February 2026).
44. Aoyama, M.; Hamajima, Y.; Hult, M.; Uematsu, M.; Oka, E.; Tsumune, D.; Kumamoto, Y. ^{134}Cs and ^{137}Cs North Pacific Ocean derived from the March 2011 TEPCO Fukushima Dai-ichi Nuclear Power Plant accident, Japan. *Oceanography* **2016**, *29*, 204–217.
45. Uddin, S.; Fowler, S.W.; Behbehani, M.; Al-Ghadban, A.N.; Swarzenski, P.W.; Al-Awadhi, N. A review of radioactivity in the Gulf region. *Mar. Pollut. Bull.* **2020**, *159*, 111481. [CrossRef] [PubMed]
46. Wada, T.; Fujita, T.; Nemoto, Y.; Shimamura, S.; Mizuno, T.; Sohtome, T.; Kamiyama, K.; Narita, K.; Watanabe, M.; Hatta, N.; et al. Effects of the nuclear disaster on marine products in Fukushima: An update after five years. *J. Environ. Radioact.* **2016**, *164*, 312–324. [CrossRef] [PubMed]
47. Men, W.; Deng, F.; He, J.; Yu, W.; Wang, F.; Li, Y.; Lin, F.; Lin, J.; Lin, L.; Zhang, Y.; et al. Radioactive impacts on nekton species in the Northwest Pacific and humans more than one year after the Fukushima nuclear accident. *Ecotoxicol. Environ. Saf.* **2017**, *144*, 601–610. [CrossRef] [PubMed]
48. Wada, T.; Konoplev, A.; Wakiyama, Y.; Watanabe, K.; Furuta, Y.; Morishita, D.; Kawata, G.; Nanba, K. Cesium radioactivity in marine and freshwater products and its relation to the restoration of fisheries in Fukushima: A decade review. In *Behavior of Radionuclides in the Environment III: Fukushima*; Nanba, K., Konoplev, A., Wada, T., Eds.; Springer: Berlin/Heidelberg, Germany, 2022.
49. Fakhri, Y.; Sarafraz, M.; Pilevar, Z.; Daraei, H.; Rahimizadeh, A.; Kazemi, S.; Khedher, K.M.; Thai, V.N.; Ba, L.H.; Khaneghah, A.M. The concentration and health risk assessment of radionuclides in the muscle of tuna fish: A worldwide systematic review and meta-analysis. *Chemosphere* **2022**, *289*, 133149. [CrossRef] [PubMed]
50. JMAFF. Japanese Ministry of Agriculture, Forestry, and Fisheries. Results of the Inspection on Radioactivity Materials in Fisheries Products. 2011. Available online: http://www.jfa.maff.go.jp/e/inspection/index.html (accessed on 13 November 2025).
51. Madigan, D.J.; Baumann, Z.; Fisher, N.S. Pacific bluefin tuna transport Fukushima-derived radionuclides from Japan to California. *Proc. Natl. Acad. Sci. USA* **2012**, *109*, 9483–9486. [CrossRef] [PubMed]
52. Povinec, P.P.; Hirose, K. Fukushima radionuclides in the NW Pacific, and assessment of doses for Japanese and world population from ingestion of seafood. *Sci. Rep.* **2016**, *5*, 9016. [CrossRef] [PubMed]
53. EUROATOM. Council Regulation (Euratom) 2016/52 of 15 January 2016—Annex I: Maximum Permitted Levels of Radioactive Contamination of Food. 2016. Available online: https://www.legislation.gov.uk/eur/2016/52/annex/I (accessed on 26 November 2025).
54. Doi, H.; Takahara, T.; Tanaka, K. Trophic Position and Metabolic Rate Predict the Long-Term Decay Process of Radioactive Cesium in Fish: A Meta-Analysis. *PLoS ONE* **2021**, *7*, e29295.
55. Carvalho, F.P. Radionuclide concentration processes in marine organisms: A comprehensive review. *J. Environ. Radioact.* **2018**, *186*, 124–130. [CrossRef] [PubMed]
56. Cook, G.T.; MacKenzie, A.B.; McDonald, P.; Jones, S.R. Remobilization of Sellafield-derived radionuclides and transport from the north-east Irish Sea. *J. Environ. Radioact.* **1997**, *35*, 227–241. [CrossRef]